

# Performance comparison of new and traditional arrangements of a dish-Stirling system

Cheng Zhang<sup>a</sup>, Yanping Zhang<sup>a,\*</sup>, Inmaculada Arauzo<sup>b</sup>, Wei Gao<sup>a</sup>, Chongzhe Zou<sup>a</sup>

<sup>a</sup>School of Energy and Power Engineering, Huazhong University of Science and Technology, Wuhan, China

<sup>b</sup>CIRCE Research Institute, University of Zaragoza, Maria de Luna, Zaragoza, Spain

## Abstract

The solar dish Stirling engine system is well known for its high light-to-electricity conversion efficiency. However, solar dish systems are not widely applied due to the limitation of dish collector size and Stirling engine size. This paper puts forward an effective way to overcome the limitation by using Stirling engine array (SEA) in the solar dish system to increase the power of Stirling engines. The performance of an SEA is affected by its connection type. To find out the influence of connection type, five basic connection types were proposed and SEA analytical models were developed based on Stirling engine model. In the engine model, non-ideal heat transfer, power losses due to pressure drop, finite speed of piston and mechanical friction, and heat losses due to internal conduction and shuttle conduction were analyzed. The model was evaluated by considering the prototype GPU-3 Stirling engine as a case study. Based on the SEA models, global efficiency and power of different connection types of SEAs with the same hot and cold flows were calculated. Effects of different factors were considered. Result shows that flow order has little influence on the SEA performance, and serial flows connection type is the best for an SEA to obtain best performance and adaptability for given heating and cooling fluids.

**Keywords:** Stirling cycle, Stirling engine model, Stirling engine array, connection type

## 1. Introduction

With the emphasis on energy and environmental impact, recently gaining attention is focused on Stirling engine for its high efficiency, low maintenance requirement, flexibility on energy sources, no pollution, low explosion risk. Due to its closed cycle, it can use almost any heat source, which makes it compatible with alternative and renewable energy sources.

The Stirling engine is widely used on solar dish system, known as dish-Stirling system. In a traditional dish-Stirling system, each Stirling engines is put on the focus of a parabolic dish to use the heat collected by the dish receiver for power generation. However, solar dish systems are not widely applied yet for its small capacity. Its capacity is mainly constrained by two factors: dish collector size and Stirling engine size. The dish size is limited for the cost and difficulty of production of large mirrors. The Stirling engine size is limited for its low power-to-weight ratio. The tracking feature of dish collector limits the weight of engine on the focal point. Besides, the size of engine is limited for it overlaps part of the collector.

This paper presents new arrangements for dish-Stirling system demonstrated in Figure 1 to solve the limitations. Stirling engines are put on the ground as a Stirling engine

array (SEA). Heat collected by multiple dish collectors, or other types of collectors, or combination of different types of collectors, even heat from different heat sources is supplied to the SEA. Since the engines are static installations on the ground where space and weight are not at a premium any more, they can reach higher capacities. They can be connected in a different connection type and their performance may be improved compared to the traditional arrangement in which they are put on the focal points of each dish collector separately.

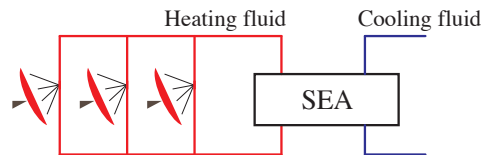


Figure 1: New arrangement of dish-Stirling system

Great attention has focused on the application using parabolic dish to collect heat. Some researchers investigated the impact of various parameters on the optical and thermal performance of the solar dish receivers using Monte Carlo Ray Tracing Method (MCRTM) and/or numerical modeling methods [1–7]. Some researchers considered the applications with different ways to use the collected heat. Loni et al. [8] considered a system using

\*Corresponding author

Email address: zyp2817@hust.edu.cn (Yanping Zhang)

parabolic dish for an organic Rankine cycle. In the proposed system, thermal oil is used as the working fluid to transport the collected heat for the organic Rankine cycle. Wang et al. [9] proposed an inverse design method for a cavity receiver used in solar dish Brayton system. Craig<sup>105</sup> et al. [10] evaluated a parabolic dish tubular receiver used in a dish Brayton cycle. An approach for incorporating a complex geometry like a tubular receiver generated using CFD software into SolTrace was developed. Aichmayer et al. [11] presented a hybrid solar micro gas-turbine system<sup>110</sup> integrating volumetric solar dish receiver. Concerning the solar dish receiver integration, both pressurized and atmospheric configurations have been considered. Lovegrove et al. [12] presented an idea of using parabolic dish array to provide heat for ammonia based thermochemical energy<sup>115</sup> storage. In this regard, using parabolic dishes to provide heat for SEA is applicable.

A large number of studies have been done on Stirling engine analysis. To describe a Stirling engine's behavior precisely is a difficult task due to the various losses and<sup>120</sup> irreversibilities in the engine. Researchers have done a lot of work to build a precise Stirling engine model. Different models of Stirling engines were developed using empirical [13–18], analytical [19–28] and numerical methods [29–39].

Among these methods, numerical methods obtain the most accurate models. Urieli and Berchowitz [29] proposed an adiabatic model of Stirling engine considering some irreversible effects such as non-ideal heat transfer processes and pressure drop effect using numerical meth-<sup>130</sup>ods. The model is known as Simple model. Many researchers developed more accurate models based on the Simple model by using alternative methods or including more loss mechanisms. Ni et al. [30] proposed an improved Simple analytical model which considers the in-<sup>135</sup>fluence mechanism of rotary speed, pressure and working gas in the view of heat/power losses for Stirling engine performance. Jia et al. [31] developed a numerical model of free-piston engine generator. The dynamic equations have been linearized to simplify the model to a<sup>140</sup> one-degree forced vibration system with various damping. The solving time of the proposed fast response model can be significantly reduced comparing to previous numerical models. Strauss and Dobson [32] proposed an alternative method to calculate the regeneration heat loss and pump-<sup>145</sup>ing losses, which is more suitable for preliminary engine design and optimisation, known as Simple II model. Abbas [33] considered the effects of non-ideal regeneration, shuttle loss and heat conduction losses based on Simple model. Araoz et al. [34] developed a rigorous Stirling en-<sup>150</sup>gine model with adiabatic working spaces, isothermal heat exchangers. It considers dead volumes, and imperfect regeneration, mechanical pumping losses due to friction, limited heat transfer and thermal losses on the heat exchangers. The model is suitable for different engine configura-<sup>155</sup>tions ( $\alpha$ ,  $\beta$  and  $\gamma$  engines). Babaelahi and Syyaadi [35] proposed a new numerical thermal model based on polytropic

expansion/compression processes. Differential equations in the expansion/compression processes were modified to polytropic processes in the new model. New model shows a better performance prediction compared with previous models.

With the development of finite-time thermodynamics, many researchers studied the the finite-time thermodynamic performance of the Stirling engine. This analysis can also be used in the case of irreversible machines further considering the internal irreversibilities of a Stirling engine such as friction, pressure drop and entropy generation [36]. Wu et al. [37] developed a numerical model considering finite-time effect to find out the relationship between the net power output and thermal efficiency of the engine. Li et al. [38] developed a mathematical model of a high temperature differential dish-Stirling system with finite-time thermodynamics. Finite-rate heat transfer, regenerative heat losses, conductive thermal bridging losses and finite regeneration processes of the Stirling engine were considered in the model. Hosseinzade [39] presented a new closed-form thermal model for the thermal simulation of Stirling engines based on the combination of polytropic analysis of expansion/compression processes and the concept of finite speed thermodynamics. Instead of finite-time method, Ahmadi et al. [40] proposed a finite-speed thermodynamic analysis based on the first law of thermodynamics for a closed system with finite speed and the direct method. The effects of heat source temperature, regenerating effectiveness, volumetric ratio, piston stroke as well as rotational speed are included in the analysis. Chen et al. [41] developed a heat-engine cycle model using finite-time thermodynamics. The model, considered the losses due to heat-resistance, heat leaks and internal irreversibility, is applicable for generalized irreversible universal steady-flow heat-engine cycles.

On the other side of the researches, multi-objective optimization algorithms were used considering multi-variables to obtain a better performance was paid for attention by numbers of researchers recently [42–45]. Ahmadi et al. [42] performed the thermodynamic analysis of solar dish Stirling engine based on the finite-time thermodynamics. Then the NSGA-II algorithm was applied. Three objectives, thermal efficiency, entransy loss rate and power output, were set as the objectives and three well known decision making methods have been employed in the algorithm. Li et al. [43] developed a multi-objective optimization model of a solar energy powered gamma type Stirling engine using Finite Physical Dimensions Thermodynamics (FPDT) method by multi-objective criteria. Genetic algorithm was used to get the Pareto frontier, and optimum points were obtained using the decision different making methods. Results show that total thermal conductance, hot temperature, stroke and diameter ratios can be improved. Patel and Savsani [44] developed a strategy for multi-objective optimization for Stirling engines using TS-TLBO (tutorial training and self learning inspired teaching-learning-based optimization) algorithm. An ap-

plication example with eleven decision variables and three objectives are considered. Luo et al. [45] proposed a multiple optimization method that combines multiple optimization algorithms including differential evolution, genetic algorithm and adaptive simulated annealing. The optimization considers five decision variables, including engine frequency, mean effective pressure, temperature of heating source, number of wires in regenerator matrix, and the wire diameter of regenerator for maximum efficiency and output power.

However, the literature review indicates that the analysis of arrangements of Stirling engines, classification and performance of the SEA, has not been reported till now. In this regard, this paper investigated the connection types of SEA and its influence on SEA performance. Connection types of SEA were classified and 5 basic connection types were put forward. According to Organ's theory [46], one equivalent analytical Stirling engine model always exists for different types ( $\alpha$  type,  $\beta$  type and  $\gamma$  type) of engines. To find out the influence of connection type of SEA and to avoid falling into the problem of developing specific Stirling engine model, a Stirling engine model based on some assumptions and simplifications was developed. This model was evaluated using experimental data of the General Motor GPU-3 Stirling engine prototype. Imperfect regeneration and some irreversibilities were considered. Heat transfer analysis of Stirling engine with heating and cooling fluids was also included. SEA models of different connection types were built depending on the engine model. Impacts of different parameters on the performance of these models were analyzed.

## 2. Connection types of SEA

For a single Stirling engine, the heat transfer processes between fluids and engine are independent and irrelevant with the direction of the flows, which means the efficiency and power are not affected by the direction of fluids. However, for an SEA, the connection type will affect the temperature profiles through the array and the specific work production, both of which will determine the efficiency and power of the SEA. It is practically significant to investigate the influence of connection type of an SEA on its performance. Then it is essential to classify the SEAs based on the connection type.

5 basic connection types of SEA were summarized according to the direction-irrelevant feature of Stirling engine, as shown in Figure 2. Type 1 is parallel flow, Type 2 is serial flows in the same order, Type 3 is serial flows in the reverse order, Type 4 is heating fluid in serial flow and cooling fluid in parallel flow and Type 5 is heating fluid in parallel flow and cooling fluid in serial flow.

All other connection types are the combination of these 5 basic connection types. For instance, an SEA in Figure 3 is the combination of Type 2 and Type 4.

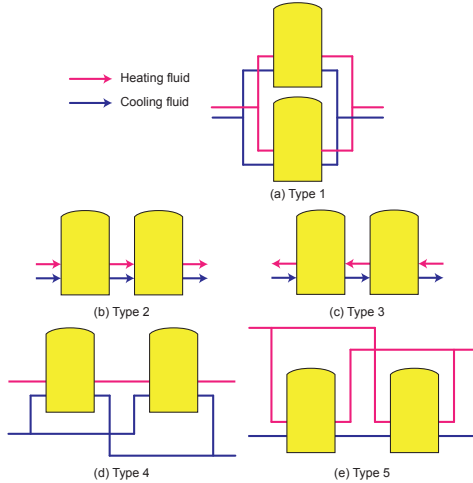


Figure 2: 5 basic connection types of SEA

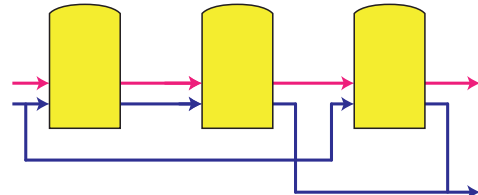


Figure 3: An instance of connection type of an SEA

## 3. Thermodynamic analysis of Stirling engine

### 3.1. Stirling engine model

#### 3.1.1. Theoretical Stirling cycle

In a Stirling cycle, there are two isothermal processes that exchange heat with heating and cooling fluids, two isochoric processes that exchange heat with regenerator. In Figure 4, the heat absorbed by regenerator in process 4-1 is reused in process 2-3, but only able to heat the working gas from 2 to 3' due to the imperfect regeneration.  $e$  is defined as the regenerator effectiveness[23, 47],  $e = \frac{T_R - T_L}{T_H - T_L}$ , where  $T_H$  is the temperature in the hot space,  $T_L$  is the temperature in the cold space,  $T_R$  is the effective working fluid temperature in the regenerator.

In order to obtain a simplified analytical model, several simplifications were made:

- The working gas in Stirling engines obeys the ideal gas law.
- No heat loss to the environment for Stirling engines.
- Overall heat transfer coefficients of the fluids are constant.
- A symmetrical regenerator behavior is assumed [23, 47] so that a simple effectiveness can be obtained by  $T_R = \frac{T_H - T_L}{\ln(T_H/T_L)}$ .

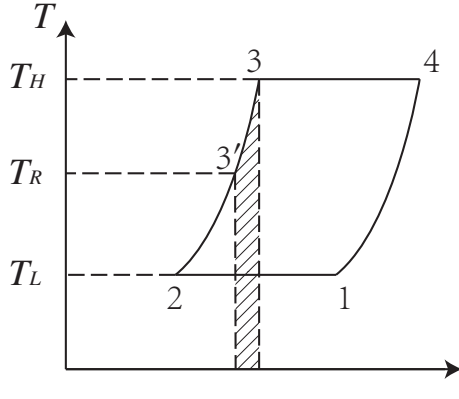


Figure 4:  $T$ - $s$  diagram of a Stirling cycle

To consider internal irreversibilities in Stirling cycle made by dead volumes, as described in [48], total dead volume  $V_D$  is divided into heater dead volume  $V_{DH}$ , regenerator dead volume  $V_{DR}$  and cooler dead volume  $V_{DC}$ . There exists a factor  $K$  to describe the dead volumes under different temperatures.  $K$  is relevant with temperatures in the process and regenerator effectiveness.

$$K = \frac{V_{DH}}{T_H} + \frac{V_{DR}}{T_R} + \frac{V_{DC}}{T_L} \quad (1)$$

For the isothermal compression process 1-2, the output work

$$W_{12} = \int_{V_E+V_C}^{V_E} p_{12} dV = -mRT_L \ln \frac{V_E + V_C + KT_L}{V_E + KT_L} \quad (2)$$

For the isothermal expansion process 3-4, the output work

$$W_{34} = \int_{V_E}^{V_E+V_C} p_{34} dV = mRT_H \ln \frac{V_E + V_C + KT_H}{V_E + KT_H} \quad (3)$$

Define  $\gamma_H = \frac{V_E + V_C + KT_H}{V_E + KT_H}$ , and  $\gamma_L = \frac{V_E + V_C + KT_L}{V_E + KT_L}$ , so in a cycle, the theoretical output work

$$W_{th} = W_{12} + W_{34} = mR(T_H \ln \gamma_H - T_L \ln \gamma_L) \quad (4)$$

For the isochoric heating process 3'-3, the absorbed heat

$$Q_{3'3} = nc_v(T_H - T_R) = \frac{1-e}{k-1} mR(T_H - T_L) \quad (5)$$

For the isothermal expansion process 3-4, the absorbed heat

$$Q_{34} = W_{34} = mRT_H \ln \gamma_H \quad (6)$$

In a cycle, the theoretical absorbed heat

$$Q_{th} = Q_{3'3} + Q_{34} = \frac{1-e}{k-1} mR(T_H - T_L) + mRT_H \ln \gamma_H \quad (7)$$

### 3.1.2. Irreversibilities and losses

#### a. Non-ideal heat transfer effect

Because of non-ideal heater and cooler, the working fluid temperature ( $T_H/T_L$ ) in these two heat exchangers is less/higher than the wall temperature ( $T_{hw}/T_{cw}$ ), respectively. And  $T_H$  and  $T_L$  can be corrected by the wall temperatures as follows:

$$T_H = T_{hw} - \frac{Q s_{se}}{h_h A_{hw}} \quad (8)$$

$$T_L = T_{cw} + \frac{(Q - W)s_{se}}{h_c A_{cw}} \quad (9)$$

The heat transfer coefficient can be obtained using the following correlation [35]:

$$h_{h,c} = \frac{\mu c_p f_{Re}}{2D_{h,c} Pr_{h,c}} \quad (10)$$

where  $f_{Re}$  is a Reynolds friction factor defined as:

$$f_{Re} = 0.0791 Re_{h,c}^{-0.75} \quad (11)$$

$Re_{h,c}$ ,  $Pr_{h,c}$  and  $D_{h,c}$  are Reynolds number, Prandtl number and hydraulic diameter of the heater/cooler exchanger.

#### b. Effect of pressure drop

Pressure drops in the heat exchangers cause power losses of the Stirling engine. The pressure drops can be obtained by [29]:

$$\Delta p = -\frac{2f_{Re}\mu u V}{d^2 A} \quad (12)$$

where  $u$  is the working gas speed,  $V$  is volume,  $A$  is flow cross-section area.

The net power loss of the Stirling engine due to pressure drop of the heat exchangers can be evaluated by:

$$W_{pd} = \oint \sum_{i=E,C} (\Delta p_i \frac{dV_i}{d\theta}) d\theta \quad (13)$$

#### c. Effect of finite speed of piston and mechanical friction

Due to the finite speed of piston, the pressure on the piston surface is different from the pressure of expansion and compression spaces. It has been demonstrated that the pressure on the piston surface in the expansion process is less than the mean pressure in the expansion space. Similarly, the pressure on the piston surface in

the compression process is greater than the mean pressure in the compression space. This means the output work is less than the theoretical value. Besides, The output work also reduces due to mechanical friction. The output work loss due to finite speed of piston and mechanical friction can be obtained as follows [35]:

$$W_{fs} = \oint p(\pm \frac{au_p}{c} \pm \frac{\Delta p_f}{p})dV \quad (14)$$

where the sign (+) is used in the compression space, and the sign (-) is used in the expansion space.  $p$  is the mean pressure in the compression/expansion space,  $u_p$  is velocity of the piston,  $c$  is the average speed of molecules and  $\Delta p_f$  is the pressure loss due to mechanical friction.  $\Delta p_f$ ,  $a$  and  $c$  can be obtained by [49]:

$$\Delta p_f = 0.97 + 0.009s_{se} \quad (15)$$

$$a = \sqrt{3k} \quad (16)$$

$$c = \sqrt{3RT} \quad (17)$$

#### d. Energy losses due to internal conduction

The temperature differs from the heater and cooler, heat losses from heater to cooler exists due to internal conduction through the walls of regenerator. [32] The internal conduction loss in a cycle can be obtained by follows:

$$Q_{id} = \frac{k_r A_r}{L_r s_{se}} (T_{hw} - T_{cw}) \quad (18)$$

where,  $k_r$ ,  $A_r$  and  $L_r$  denote the regenerator matrix conductivity, regenerator length, and regenerator conductive area respectively.

#### e. Energy losses due to shuttle conduction

The displacer shuttles between the expansion and compression space. It absorbs heat during the hot end of its stroke and releases it during the cold end of its stroke. This heat loss can be estimated as [50]:

$$Q_{sc} = 0.4 \frac{Z^2 k_p D_p}{J L_d s_{se}} (T_H - T_L) \quad (19)$$

where,  $Z$ ,  $k_p$ ,  $D_p$ ,  $J$  and  $L_d$  denote the displacer stroke, piston thermal conductivity, displacer diameter, gap between the displacer and the cylinder, and length of the displacer respectively.

So, in a Stirling engine, the total absorbed heat in a cycle

$$Q = Q_{th} + Q_{id} + Q_{sc} \quad (20)$$

the output work

$$W = W_{th} - W_{pd} - W_{fs} \quad (21)$$

Power of the Stirling engine

$$P = W s_{se} \quad (22)$$

Efficiency of the Stirling engine

$$\eta = W/Q \quad (23)$$

### 3.2. Model validation

Evaluation of the developed thermal model was performed by considering the GPU-3 Stirling engine as a case study. Design specifications of the GPU-3 Stirling engine are indicated in Table 1. The thermal efficiency and power of the proposed Stirling engine model was compared with previous thermal models and experimental data as shown in Table 2 and Table 3.

It can be found that the proposed model has much better agreement with the experimental results than previous thermal models at various rotation speeds and mean effective pressures. It is required to mention that in all thermal models both power  $W$  and input heat  $Q$  were determined by the thermal process of heat transfer between the wall and working gas. In the proposed model,  $W$  and  $Q$  are obtained by Equation 8 and 9. Therefore all the three parameters  $W$ ,  $Q$  and  $\eta$  are determined by the thermal model and input parameters to the model. These input parameters includes heater, cooler, mean effective pressure, type of working gas and geometrical specification of the engine.

Table 2 and 3 indicate that when mean effective pressure of the engine increases from 2.76 MPa to 6.90 MPa, best performance (efficiency and power) prediction of the proposed model exists. When rotation speed increases from 16.67 Hz to 58.33 Hz, error in prediction of performance of the proposed model increases. The proposed model may have the best performance prediction at a low rotation speed, with mean effective pressure between 4.14 MPa and 5.52 MPa.

However, there is still some discrepancy between the simulation results of proposed model and the experimental data. In the future researches, more accurate models of Stirling engine may be developed by considering other irreversibilities such as heat loss to the environment, gas spring hysteresis, and etc. It is worth pointing that there are more accurate Stirling engine models. For example, polytropic simulation models of Stirling engine show higher accuracy than our proposed model [35, 39]. However, the model needs more costly calculations and the polytropic indexes are engine-specific.

### 3.3. Heat transfer between the engine and the fluids

For a Stirling engine thermal process, the wall temperatures of the heater and cooler are considered to be uniform and constant. The heat transferred between the wall and the fluids is

$$(T_w - T) U dA = q_m c_p dT \quad (24)$$

with  $T(0) = T_i$ ,  $T(A) = T_o$ ,

$$\frac{T_o - T_w}{T_i - T_w} = \exp\left(-\frac{UA}{q_m c_p}\right) \quad (25)$$

For a Stirling engine,  $T_{hw}$  or  $T_{cw}$  can be used to substitute  $T_w$  to get the relationships between  $T_{i,h}$ ,  $T_{o,h}$  and  $T_{hw}$ , or  $T_{i,c}$ ,  $T_{o,c}$  and  $T_{cw}$  respectively.

Table 1: Design specifications of the GPU-3 Stirling engine [35, 51]

Parameter	Value
Engine type	$\beta$
Working gas	Helium
Mass of the working gas	1.136 g
<i>Heater</i>	
Number of tubes	40
Tube external diameter	$4.83 \times 10^{-3}$ m
Tube internal diameter	$3.02 \times 10^{-3}$ m
Tube length (cylinder side)	0.1164 m
Tube length (regenerator side)	0.1289 m
<i>Cooler</i>	
Number of tubes	312
Tube external diameter	$1.59 \times 10^{-3}$ m
Tube internal diameter	$1.09 \times 10^{-3}$ m
Average tube length	$4.61 \times 10^{-2}$ m
<i>Regenerator</i>	
Number of regenerator	8
Regenerator internal diameter	$2.26 \times 10^{-2}$ m
Regenerator length	$2.26 \times 10^{-2}$ m
Diameter of regenerator tube	$4 \times 10^{-5}$ m
Material	Stainless steel
<i>Volume</i>	
Swept Vol. (expansion/compression)	120.82/114.13 cm <sup>3</sup>
Clearance Vol. (expansion/compression)	30.52/28.68 cm <sup>3</sup>
Dead Vol. (heater/cooler/regenerator)	70.28/13.18/50.55 cm <sup>3</sup>

Table 2: Thermal efficiency of the proposed Stirling engine model, previous thermal models and experimental data(at  $T_{hw} = 922$  K and  $T_{cw} = 288$  K)

Rotation speed (Hz)	Mean effective pressure (MPa)	Thermal efficiency predicted by the simple analysis (variable Pr [29])			Thermal efficiency predicted by the adiabatic analysis (simple II [32])			Thermal efficiency predicted by the proposed Stirling Engine model			Experimental efficiency [35]
		Value (%)	Error (%)	Average error (%)	Value (%)	Error (%)	Average error (%)	Value (%)	Error (%)	Average error (%)	
16.67	2.76	38.72	18.22		32.48	11.98		28.16	7.66		20.50
25.00		36.16	15.46		31.21	10.51		27.75	7.05		20.70
33.33		33.79	15.79	17.90	29.45	11.45	12.85	27.43	9.43	12.10	18.00
41.67		31.48	16.28		27.45	12.25		27.17	11.97		15.20
50.00		29.12	17.32		25.21	13.41		26.94	15.14		11.80
58.33		29.74	24.34		22.89	17.49		26.74	21.34		5.40
25.00	4.14	35.65	10.85		32.29	7.49		27.29	2.49		24.80
33.33		33.52	9.62		30.40	6.50		26.94	3.04		23.90
41.67		31.48	10.18	11.46	28.39	7.09	8.28	26.65	5.35	6.65	21.30
50.00		29.45	11.25		26.33	8.13		26.39	8.19		18.20
58.33		27.40	15.40		24.21	12.21		26.17	14.17		12.00
41.67	5.52	31.20	8.70		28.59	6.09		26.24	3.74		22.50
50.00		29.33	10.53	10.82	26.62	7.82	8.11	25.97	7.17	7.48	18.80
58.33		27.44	13.24		24.62	10.42		25.73	11.53		14.20
50.00	6.90	29.07	10.37	11.73	26.61	7.91	9.19	25.62	6.92	9.05	18.70
58.33		27.29	13.09		24.67	10.47		25.37	11.17		14.20

Table 3: Output power of the proposed Stirling engine model, previous thermal models and experimental data(at  $T_{hw} = 922$  K and  $T_{cw} = 288$  K)

Rotation speed (Hz)	Mean effective pressure (MPa)	Output power predicted by the simple analysis (variable Pr [29])			Output power predicted by the adiabatic analysis (simple II [32])			Output power predicted by the proposed Stirling Engine model			Experimental output power (kW) [35]
		Value (kW)	Error (%)	Average error (%)	Value (kW)	Error (%)	Average error (%)	Value (kW)	Error (%)	Average error (%)	Actual value (kW)
16.67	2.76	1.796	119.02		1.772	116.10		0.861	4.98		0.82
25.00		2.555	128.13		2.500	123.21		1.253	11.88		1.12
33.33		3.215	165.70	272.03	3.117	157.60	254.71	1.632	34.88	104.84	1.21
41.67		3.769	211.49		3.615	198.76		2.001	65.37		1.21
50.00		4.195	303.37		3.973	282.08		2.362	127.12		1.04
58.33		4.505	704.46		4.203	650.54		2.715	384.82		0.56
25.00	4.14	3.844	114.75		3.761	110.11		1.818	1.56		1.79
33.33		4.856	120.73		4.708	114.00		2.362	7.36		2.20
41.67		5.734	136.94	259.70	5.501	127.31	158.41	2.890	19.42	39.83	2.42
50.00		6.462	174.98		6.126	160.68		3.405	44.89		2.35
58.33		7.030	306.36		6.573	279.94		3.908	125.90		1.73
41.67	5.52	7.645	133.08		7.334	123.60		3.742	14.09		3.28
50.00		8.655	163.87	180.02	8.206	150.18	164.91	4.401	34.18	43.68	3.28
58.33		9.470	243.12		8.858	220.94		5.045	82.79		2.76
50.00	6.90	10.788	174.50	287.04	10.223	160.13	263.63	5.362	36.44	97.75	3.93
58.33		11.840	399.58		11.071	367.13		6.140	159.07		2.37

$$\frac{T_{o,h} - T_{hw}}{T_{i,h} - T_{hw}} = \exp\left(-\frac{U_h A_h}{q_{m,h} c_{p,h}}\right) \quad (26)$$

$$\frac{T_{o,c} - T_{cw}}{T_{i,c} - T_{cw}} = \exp\left(-\frac{U_c A_c}{q_{m,c} c_{p,c}}\right) \quad (27)$$

preferred. Air is chosen as the cooling fluid instead of commonly used water to avoid small temperature rise and evaporation after the cooling process. Chosen parameters of Stirling engines and heating/cooling fluids in SEAs are shown in Table 4.

Table 4: Parameters of SEA models

Parameter	Value	Parameter	Value
Heating fluid	Air	$q_{m,h}$	0.4 kg/s
Cooling fluid	Air	$T_{i,h}$	1000 K
$n_{se}$	6	$p_{i,h}$	$5 \times 10^5$ Pa
$s_{se}$	25 Hz	$q_{m,c}$	0.4 kg/s
$p_{se}$	5 MPa	$T_{i,c}$	300 K
$U_h A_h$	180 W/K	$p_{i,c}$	$5 \times 10^5$ Pa
$U_c A_c$	180 W/K		

Heat transferred from heating fluid to Stirling engine in a cycle

$$q_{m,h} c_{p,h} (T_{i,h} - T_{o,h}) / s_{se} = Q \quad (28)$$

Heat transferred from Stirling engine to cooling fluid in a cycle

$$q_{m,c} c_{p,c} (T_{o,c} - T_{i,c}) / s_{se} = Q - W \quad (29)$$

#### 4. Modeling of the SEAs

To determine the performance of an SEA, models of all the Stirling engines need to be built depending on their thermodynamic characteristic. Stirling engines are chosen to have the same parameters including the same speed  $s_{se}$ . This is especially practical when using SEA for power generation, where the output power frequency should be constant. The speed of Stirling engine can be calibrated by speed controller system [52]. To eliminate interference of other factors, heating and cooling fluids are chosen to have same parameters for different connection types of SEAs. To clearly find out the performance differences of different SEAs, large temperature differences of the heating/cooling fluids after heat exchange with the engines are

In an SEA, there are 2 flows as shown in Figure 2. In a serial flow, each engine's mass flow rate is  $q_m$ , and from the flow's direction, for  $2 \leq x \leq n_{se}$ ,  $T_{i,x} = T_{o,x-1}$ . In a parallel flow, each engine's mass flow is  $q_m/n_{se}$ , for  $2 \leq x \leq n_{se}$ ,  $T_{i,x} = T_{i,h}$ .

MATLAB was used as the programming tool to build the model of SEAs, and CoolProp was used to provide fluid properties for MATLAB program. 5 basic SEA models composed of the aforementioned Stirling engines and fluids were built. To compare SEA connection types under various conditions, several parameters are investigated to find out their effects on SEA performance.

Figure 5 shows the solution algorithm of the SEA model. As it is shown, known inlet parameters of the fluids, the performance of a Stirling engine can be obtained from flowchart (a) according to the equations derived; similarly, known inlet parameters of heating fluid and outlet parameters of cooling fluid, the performance of a Stirling engine can be obtained from flowchart (b). Flowchart (c) shows the algorithm to solve the SEA model iteratively depending on different connection types. The levenberg-marquardt algorithm is applied to numerically solve the non-linear equations in the flowcharts.

### 5.2. Effects of $q_m c_p$

According to Equation 28, 29,  $q_m c_p$  (both  $q_{m,h} c_{p,h}$  and  $q_{m,c} c_{p,c}$ ) will affect the heat transfer process, which is one of the vital factor for the performance of SEA.

Curves of performance of SEAs and  $q_{m,h} c_{p,h}$  are shown in Figure 7. For a large  $q_{m,h} c_{p,h}$  ( $> 800 \text{ W/K}$ ), Type 2, Type 3 and Type 5 have similar performance, which can be interpreted as the cooling fluid has the same properties for the two types of SEAs, and for a large  $q_{m,h} c_{p,h}$ , the heating fluid has similar effect after diverged. Similar performance of Type 1 and Type 4 can be also interpreted for the same reason.

## 5. Result Analysis

SEA models with specified parameters in Table 4 were built and calculated. Results are shown in Table 5, it can be found that under specified parameters Type 3 has the highest efficiency and output power, while Type 1 has the lowest efficiency and output power.

Table 5: Results of SEA models under specified parameters

Parameter	Value	Parameter	Value
$\eta_1$	0.2215	$P_1$	8022 W
$\eta_2$	0.2273	$P_2$	8483 W
$\eta_3$	0.2277	$P_3$	8512 W
$\eta_4$	0.2227	$P_4$	8116 W
$\eta_5$	0.2263	$P_5$	8399 W

### 5.1. Effects of $T_{i,h}$

According to Carnot cycle efficiency formula, the temperature of heating fluid determines the efficiency of Stirling engine array. For a Stirling engine, lower temperature heating fluid leads to a lower efficiency. The efficiency and output power may drop to 0 due to its insufficient heating fluid temperature to drive the engine.

Curves of performance of SEAs and  $T_{i,h}$  are shown in Figure 6. As it is shown, with the increase of  $T_{i,h}$ , both  $\eta$  and  $P$  increase for all SEAs. For some types of SEA, when  $T_{i,h}$  is lower than a critical temperature, some of the engines in the SEA will not work and there will be turning points on the  $\eta - T_{i,h}$ ,  $P - T_{i,h}$  curves. E.g. for SEA of Type 1, when  $T_{i,h}$  is lower 820 K, all the engines stop working, turning points at 820 K can be found on the  $\eta - T_{i,h}$ ,  $P - T_{i,h}$  curves in Figure 6.

From curves in Figure 6, it can be concluded that Type 2 and Type 3 have the best performance, and Type 2 has the best adaptability for lower  $T_{i,h}$ . All engines in Type 2 begin to work at 730 K.

Curves of performance of SEAs and  $q_{m,c} c_{p,c}$  are shown in Figure 8. For a connection type of SEA, the performance improves with the increase of  $q_{m,c} c_{p,c}$ . For a large  $q_{m,c} c_{p,c}$  ( $> 800 \text{ W/K}$ ), Type 2 and Type 3 have similar performance, which means the flow order doesn't affect the performance of SEA with a large  $q_{m,c} c_{p,c}$ . There exists an intersection point (at 830 W/K) of curves of Type 4 and Type 5. For a larger  $q_{m,c} c_{p,c}$ , Type 4 has a better performance, and vice versa. This can be interpreted that larger  $q_{m,c} c_{p,c}$  weaken the drawback of larger temperature rise of parallel flow, while for the heating fluid, temperature drop of serial flow is smaller than parallel flow.

### 5.3. Effects of $n_{se}$

By varying the number of engines in SEA, the performance levels changed accordingly.  $n_{se}$  may affect both the flow rates and temperatures of fluids of each engine. Figure 9 shows curves of performance of SEAs with different  $n_{se}$ . As it is shown, with an increase of  $n_{se}$  leads to a reduction of  $\eta$  for all SEAs due to smaller heating and cooling average temperature difference for more engines. For some types of SEA, when  $n_{se}$  is larger than a critical value, some of the engines in the SEA will not work and the curves will dive. E.g. for SEA of Type 1, when  $n_{se}$  is larger than 9, all the engines stop working, turning points at 9 can be found on the  $\eta - n_{se}$ ,  $P - n_{se}$  curves in Figure 9.

For Type 1, when  $n_{se} \geq 10$ , all engines stop working for given heating and cooling fluids due to small  $q_m c_p$ . For Type 2 and Type 3, every engine in the SEAs works, by increasing  $n_{se}$ ,  $\eta$  reduces due to smaller temperature difference of the fluids, and  $P$  increases due to more operating engines. For Type 4, by checking results, it can be found that when  $n_{se} = 13$ , the last engine doesn't work; when  $n_{se} = 14$ , only the first 10 engines will work; when  $n_{se} = 15$ , the working engine number drops to 9. For Type 5, by checking results, it can be found that when  $n_{se} = 12$ , the last 2 engines stop working; when  $n_{se} = 13$ , only the first 8 engines will work; when  $n_{se} = 14$ , the working engine number drops to 6; when  $n_{se} = 15$ , the working engine number drops to 4.

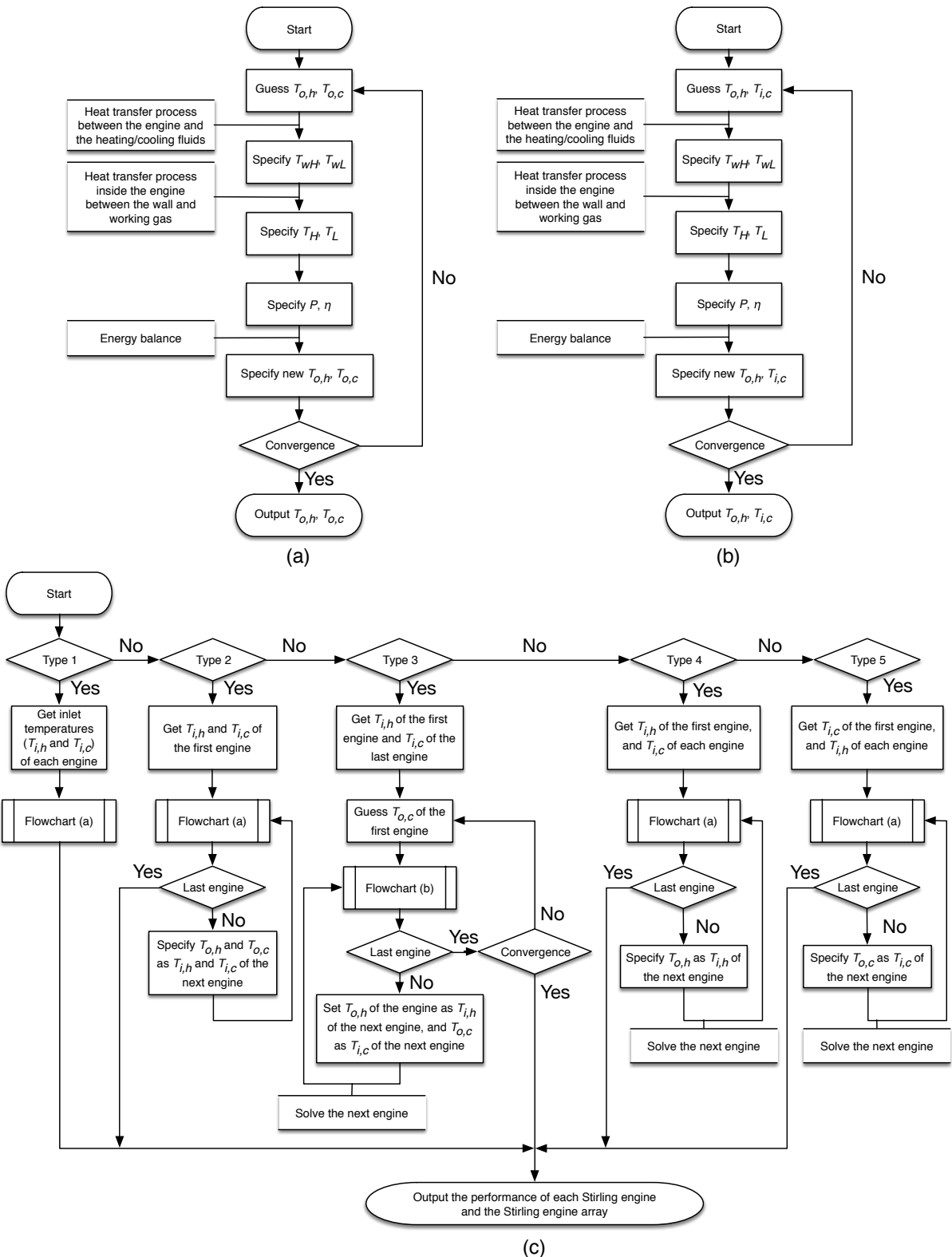


Figure 5: Flowchart of the SEA model for performance analysis of the SEAs

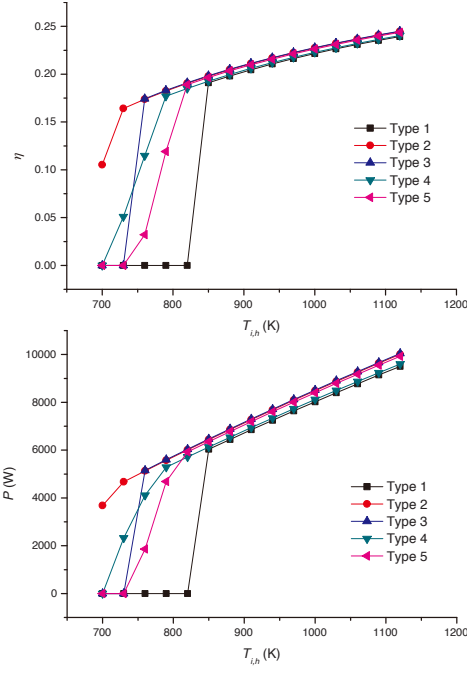


Figure 6: Influence of  $T_{i,h}$  on efficiency and power of SEA

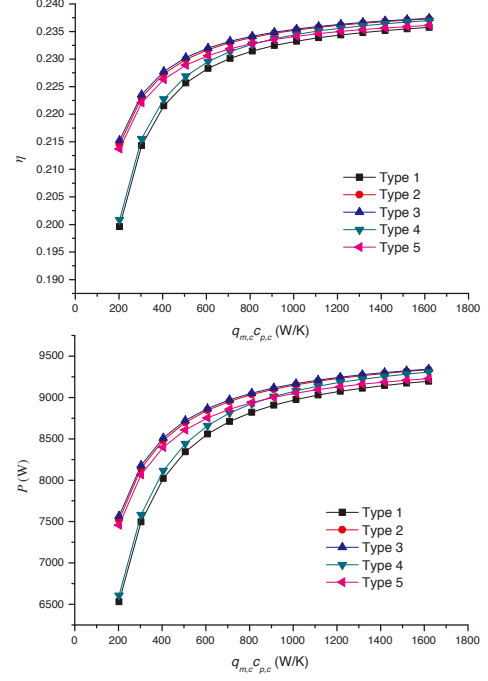


Figure 8: Influence of  $q_{m,c} c_{p,c}$  on efficiency and power of SEA

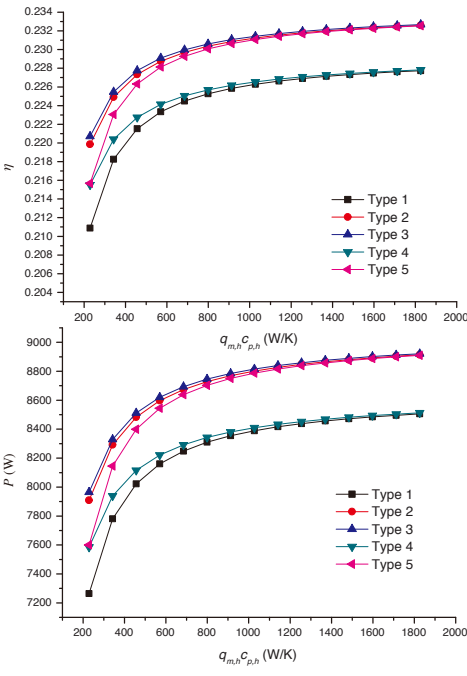


Figure 7: Influence of  $q_{m,h} c_{p,h}$  on efficiency and power of SEA

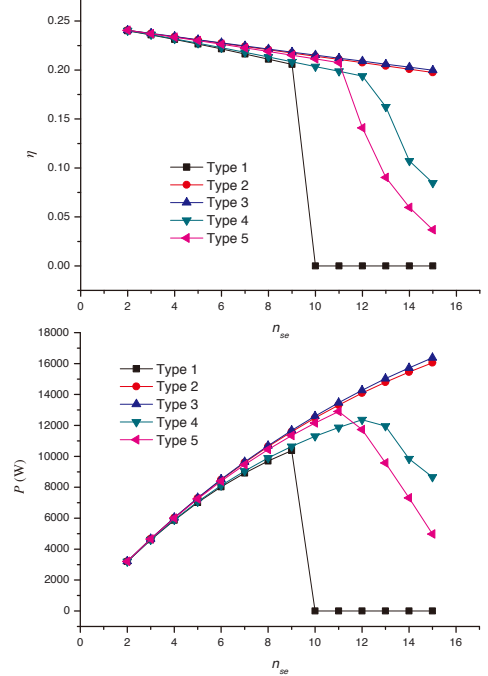


Figure 9: Influence of  $n_{se}$  on efficiency and power of SEA

## 6. Conclusion

Connection type may change the flow rates and temperatures of the fluids, as a result the performance of the SEA will be different depending on the connection schemes. In order to compare performance of SEAs with different connections, five basic connection types of SEA were summed up according to flow type and flow order.

Analytical Stirling engine model was created to develop the SEA models for the investigation of influence of connection types. Imperfect regeneration and cycle irreversibility of Stirling engine cycle and heat exchange process between fluids and engine were considered in the model. The model was evaluated by considering the prototype GPU-3 Stirling engine as a case study. Result shows that the proposed model predicted the performance with higher accuracy than the previous models. Models of SEAs were developed to calculate the performance under different parameters to find out impacts of  $T_{i,h}$ ,  $q_{m,h}c_{p,h}$ ,  $q_{m,c}c_{p,c}$  and  $n_{se}$  on different connection types.

It was found that, as expected, decrease  $T_{i,h}$  and  $q_{m,c}c_p$  will weaken the performance of SEA of all connection types. However, for some connection types, there exists a critical temperature below which some engines stop working. This needs to be considered for SEA connection type selection, especially when  $T_{i,h}$  is low. For given  $T_{i,h}$ ,  $T_{i,c}$  and  $q_{m,c}c_p$ , Type 2 has the best performance and adaptability.

From Figure 6-9, it can be found that Type 2 and Type 3 have the best performance, while Type 1 has the worst performance. Type 2 and Type 3 have similar performance under different parameters ( $T_{i,h}$ ,  $T_{i,c}$  and  $q_{m,c}c_p$ ), which means the flow order has little influence on the performance of an SEA.

For a certain connection type, increase  $n_{se}$  will reduce the efficiency of SEA. For some connection types, increase  $n_{se}$  will reduce the output power  $P$  due to inoperative engines and smaller output power engines. Thus it is important to choose the number of engines for some connection types of SEA.

As a conclusion, SEA of serial flows has the best performance and adaptability under different parameters. Given heating and cooling fluids, using serial flow is the best choice for the connection type of an SEA.

It is important to note that, in the future researches, the experiments of influence of connection type on SEA's performance can be carried out to verify the conclusions in this paper.

## Acknowledgement

We gratefully acknowledge the support of International S&T Cooperation Program of China, under Grant No. 2014DFA60990, without which the present study could not have been completed.

555	<b>Nomenclature</b>	590	$\gamma_L$	space ratio in process 34
	$A$ heat transfer area ( $\text{m}^2$ )		$\mu$	dynamic viscosity ( $\text{kg} \cdot \text{m}^{-1} \cdot \text{s}^{-1}$ )
	$c_p$ specific heat at constant pressure ( $\text{J} \cdot \text{kg}^{-1} \cdot \text{K}^{-1}$ )			<b>Subscripts</b>
	$c_v$ specific heat at constant volume ( $\text{J} \cdot \text{kg}^{-1} \cdot \text{K}^{-1}$ )		$c$	cooling fluid
	$e$ regenerator effectiveness		$cw$	cooler wall
560	$J$ annular gap cylinder displacer (m)	595	$h$	heating fluid
	$K$ dead volume factor		$hw$	heater wall
	$k$ specific heat ratio ( $c_p/c_v$ ), thermal conductivity ( $\text{W} \cdot \text{m}^{-1} \cdot \text{K}^{-1}$ )		$i$	inlet
	$m$ mass of working fluid in Stirling engine (kg)		$o$	outlet
565	$n_{se}$ number of Stirling engine in SEA	600	$p$	piston
	$P$ power of Stirling engine (W)		$r$	regenerator
	$p$ pressure (Pa)		$th$	theoretical
	$Q$ absorbed heat (J)			
	$q_m$ mass flow rate ( $\text{kg} \cdot \text{s}^{-1}$ )			
570	$R$ gas constant ( $\text{J} \cdot \text{kg}^{-1} \cdot \text{K}^{-1}$ )			
	$s_{se}$ speed of Stirling engine (Hz)			
	$T_H$ working fluid temperature in the hot space (K)			
	$T_L$ working fluid temperature in the cold space (K)			
	$T_R$ effective working fluid temperature in regenerator (K)			
575	$T_w$ wall temperature (K)			
	$U$ overall heat transfer coefficient ( $\text{W} \cdot \text{m}^{-2} \cdot \text{K}^{-1}$ )			
	$V_C$ compression volume ( $\text{m}^3$ )			
	$V_D$ total dead volume ( $\text{m}^3$ )			
580	$V_E$ expansion volume ( $\text{m}^3$ )			
	$V_{DC}$ cold space dead volume ( $\text{m}^3$ )			
	$V_{DH}$ hot space dead volume ( $\text{m}^3$ )			
	$V_{DR}$ regenerator dead volume ( $\text{m}^3$ )			
	$W$ output work (J)			
585	$Z$ displacer stroke (m)			

### Abbreviations

SEA Stirling engine array

### Greek Symbols

$\gamma_H$  space ratio in process 12

- [1] Z.D. Cheng, Y.L. He, and F.Q. Cui. A new modelling method and unified code with mcrt for concentrating solar collectors and its applications. *Applied Energy*, 101:686 – 698, 2013. Sustain-<sup>675</sup>able Development of Energy, Water and Environment Systems.
- [2] Mao Qianjun, Xie Ming, Shuai Yong, and Yuan Yuan. Study on solar photo-thermal conversion efficiency of a solar parabolic dish system. *Environmental Progress & Sustainable Energy*, 33(4):1438–1444, 2014.
- [3] Mo Wang and Kamran Siddiqui. The impact of geometrical parameters on the thermal performance of a solar receiver of dish-type concentrated solar energy system. *Renewable Energy*, 35(11):2501 – 2513, 2010.
- [4] Fuqiang Wang, Yong Shuai, Heping Tan, Xiaofeng Zhang, and Qianjun Mao. Heat transfer analyses of porous media receiver with multi-dish collector by coupling mcrt and fvm method. *Solar Energy*, 93:158 – 168, 2013.
- [5] Jianqin Zhu, Kai Wang, Hongwei Wu, Dunjin Wang, Juan Du, and A.G. Olabi. Experimental investigation on the energy and exergy performance of a coiled tube solar receiver. *Applied Energy*, 156:519 – 527, 2015.
- [6] Sha Li, Guoqiang Xu, Xiang Luo, Yongkai Quan, and Yunting Ge. Optical performance of a solar dish concentrator/receiver system: Influence of geometrical and surface properties of cavity receiver. *Energy*, 113:95 – 107, 2016.
- [7] Ahmed M. Daabo, Saad Mahmoud, and Raya K. Al-Dadah. The effect of receiver geometry on the optical performance of a small-scale solar cavity receiver for parabolic dish applications. *Energy*, 114:513 – 525, 2016.
- [8] R. Loni, A.B. Kasaeian, E. Askari Asli-Ardeh, B. Ghobadian, and W.G. Le Roux. Performance study of a solar-assisted organic rankine cycle using a dish-mounted rectangular-cavity tubular solar receiver. *Applied Thermal Engineering*, 108:1298 – 1309, 2016.
- [9] Wujun Wang, Haoxin Xu, Björn Laumert, and Torsten Strand. An inverse design method for a cavity receiver used in solar dish brayton system. *Solar Energy*, 110:745 – 755, 2014.
- [10] Ken J. Craig, Justin Marsberg, and Josua P. Meyer. Combining ray tracing and cfd in the thermal analysis of a parabolic dish<sup>710</sup> tubular cavity receiver. *AIP Conference Proceedings*, 1734(1), 2016.
- [11] Lukas Aichmayer, James Spelling, and Bjrn Laumert. Preliminary design and analysis of a novel solar receiver for a micro gas-turbine based solar dish system. *Solar Energy*, 114:378 – 396, 2015.
- [12] K Lovegrove, A Luzzi, I Soldiani, and H Kreetz. Developing ammonia based thermochemical energy storage for dish power plants. *Solar Energy*, 76(1–3):331 – 337, 2004. Solar World Congress 2001.
- [13] James R. Senft. Theoretical limits on the performance of stirling engines. *International Journal of Energy Research*, 22(11):991–1000, 9 1998.
- [14] M. Costea, S. Petrescu, and C. Harman. The effect of irreversibilities on solar stirling engine cycle performance. *Energy<sup>725</sup> Conversion and Management*, 40(15–16):1723 – 1731, 1999.
- [15] J I Prieto and A B Stefanovskiy. Dimensional analysis of leakage and mechanical power losses of kinematic stirling engines. *Proceedings of the Institution of Mechanical Engineers, Part C: Journal of Mechanical Engineering Science*, 217(8):917–934,<sup>730</sup> 2003.
- [16] Allan J. Organ. *Stirling Cycle Engines : Inner Workings and Design (1)*. Wiley, Somerset, GB, 2013.
- [17] Bancha Kongtragool and Somchai Wongwises. Investigation on power output of the gamma-configuration low temperature differential stirling engines. *Renewable Energy*, 30(3):465 – 476, 2005.
- [18] D.G. Thombare and S.K. Verma. Technological development in the stirling cycle engines. *Renewable and Sustainable Energy Reviews*, 12(1):1 – 38, 2008.
- [19] Michihiro Ohtomo and Naotsugu Isshiki. Basic performance of a three-temperature stirling cycle machine using vector analysis. *Nihon Kikai Gakkai Ronbunshu B Hen/transactions of the Japan Society of Mechanical Engineers Part B*, 61(591):4219–4225, 1995.
- [20] E.D. Rogdakis, N.A. Bormpilas, and I.K. Koniakos. A thermodynamic study for the optimization of stable operation of free piston stirling engines. *Energy Conversion and Management*, 45(4):575 – 593, 2004.
- [21] Bancha Kongtragool and Somchai Wongwises. Thermodynamic analysis of a stirling engine including dead volumes of hot space, cold space and regenerator. *Renewable Energy*, 31(3):345 – 359, 2006.
- [22] Pascal Puech and Victoria Tishkova. Thermodynamic analysis of a stirling engine including regenerator dead volume. *Renewable Energy*, 36(2):872 – 878, 2011.
- [23] F. Formosa and G. Despesse. Analytical model for Stirling cycle machine design. *Energy Conversion and Management*, 51(10):1855–1863, 2010.
- [24] J.H. Shazly, A.Z. Hafez, E.T. El Shenawy, and M.B. Eteiba. Simulation, design and thermal analysis of a solar stirling engine using matlab. *Energy Conversion and Management*, 79:626 – 639, 2014.
- [25] Barry Cullen and Jim McGovern. Development of a theoretical decoupled stirling cycle engine. *Simulation Modelling Practice and Theory*, 19(4):1227 – 1234, 2011. Sustainable Energy and Environmental Protection “SEEP2009”.
- [26] Mohammad Hossein Ahmadi, Hoseyn Sayyaadi, Saeed Dehghani, and Hadi Hosseinzade. Designing a solar powered stirling heat engine based on multiple criteria: Maximized thermal efficiency and power. *Energy Conversion and Management*, 75:282 – 291, 2013.
- [27] Mohammad H. Ahmadi, Hoseyn Sayyaadi, Amir H. Mohammadi, and Marco A. Barranco-Jimenez. Thermo-economic multi-objective optimization of solar dish-stirling engine by implementing evolutionary algorithm. *Energy Conversion and Management*, 73:370 – 380, 2013.
- [28] I. A. Tursunbaev. Analytic model of solar power plant with a stirling engine. *Applied Solar Energy*, 43(1):13–16, 03 2007. - Allerton Press, Inc. 2007; - 2014-08-30.
- [29] Israel Urieli and David M. Berchowitz. *Stirling cycle engine analysis*. A. Hilger, Bristol, 1984.
- [30] Mingjiang Ni, Bingwei Shi, Gang Xiao, Hao Peng, Umair Sultan, Shurong Wang, Zhongyang Luo, and Kefa Cen. Improved simple analytical model and experimental study of a 100 w betatype stirling engine. *Applied Energy*, 169:768 – 787, 2016.
- [31] Boru Jia, Andrew Smallbone, Huihua Feng, Guohong Tian, Zhengxing Zuo, and A.P. Roskilly. A fast response free-piston engine generator numerical model for control applications. *Applied Energy*, 162:321 – 329, 2016.
- [32] Johannes M. Strauss and Robert T. Dobson. Evaluation of a second order simulation for sterling engine design and optimisation. *Journal of Energy in Southern Africa*, 21(2):17–29, 2010.
- [33] Mohamed Abbas. Thermal analysis of stirling engine solar driven. *Cder Dz*, 70(3):503–514, 2014.
- [34] Joseph A. Araoz, Marianne Salomon, Lucio Alejo, and Torsten H. Fransson. Numerical simulation for the design analysis of kinematic stirling engines. *Applied Energy*, 159:633 – 650, 2015.
- [35] Mojtaba Babaehli and Hoseyn Sayyaadi. A new thermal model based on polytropic numerical simulation of stirling engines. *Applied Energy*, 141:143 – 159, 2015.
- [36] Germilly Barreto and Paulo Canhoto. Modelling of a stirling engine with parabolic dish for thermal to electric conversion of solar energy. *Energy Conversion and Management*, 132:119 – 135, 2017.
- [37] Feng Wu, Lingen Chen, Chih Wu, and Fengrui Sun. Optimum performance of irreversible stirling engine with imperfect regeneration. *Energy Conversion and Management*, 39(8):727 – 732, 1998.
- [38] Li Yaqi, He Yaling, and Wang Weiwei. Optimization of solar-powered stirling heat engine with finite-time thermodynamics. *Renewable Energy*, 36(1):421 – 427, 2011.
- [39] Hadi Hosseinzade, Hoseyn Sayyaadi, and Mojtaba Babaehli.

- 745 A new closed-form analytical thermal model for simulating stirling engines based on polytropic-finite speed thermodynamics. *Energy Conversion and Management*, 90:395 – 408, 2015.
- [40] Mohammad H. Ahmadi, Mohammad Ali Ahmadi, Fathollah Pourfayaz, Mokhtar Bidi, Hadi Hosseinzade, and Michel Feidt. Optimization of powered stirling heat engine with finite speed thermodynamics. *Energy Conversion and Management*, 108:96 – 105, 2016.
- 750 [41] Lingen Chen, Wanli Zhang, and Fengrui Sun. Power, efficiency, entropy-generation rate and ecological optimization for a class of generalized irreversible universal heat-engine cycles. *Applied Energy*, 84(5):512 – 525, 2007.
- 755 [42] Mohammad Hossein Ahmadi, Mohammad Ali Ahmadi, Adel Mellit, Fathollah Pourfayaz, and Michel Feidt. Thermodynamic analysis and multi objective optimization of performance of solar dish stirling engine by the centrality of entransy and entropy generation. *International Journal of Electrical Power & Energy Systems*, 78:88 – 95, 2016.
- 760 [43] Ruijie Li, Lavinia Grosu, and Diogo Queiros-Conde. Multi-objective optimization of stirling engine using finite physical dimensions thermodynamics (fpdt) method. *Energy Conversion and Management*, 124:517 – 527, 2016.
- 765 [44] Vivek Patel and Vimal Savsani. Multi-objective optimization of a stirling heat engine using ts-tlbo (tutorial training and self learning inspired teaching-learning based optimization) algorithm. *Energy*, 95:528 – 541, 2016.
- 770 [45] Zhongyang Luo, Umair Sultan, Mingjiang Ni, Hao Peng, Bingwei Shi, and Gang Xiao. Multi-objective optimization for gpu<sup>3</sup> stirling engine by combining multi-objective algorithms. *Renewable Energy*, 94:114 – 125, 2016.
- 775 [46] Allan J. Organ. The regenerator and the stirling engine. *Mechanical Engineering Publications Limited*, 1997.
- [47] A.J. Juhasz. A mass computation model for lightweight brayton cycle regenerator heat exchangers. In *8th Annual International Energy Conversion Engineering Conference*, 2010.
- 780 [48] Chen Duan, Xinggang Wang, Shuiming Shu, Changwei Jing, and Huawei Chang. Thermodynamic design of stirling engine using multi-objective particle swarm optimization algorithm. *Energy Conversion & Management*, 84:88–96, 2014.
- 785 [49] Heywood and JohnB. *Internal combustion engine fundamentals*. McGraw-Hill, 1988.
- [50] Youssef Timoumi, Iskander Tili, and Sassi Ben Nasrallah. Design and performance optimization of gpu-3 stirling engines. *Energy*, 33(7):1100 – 1114, 2008.
- 790 [51] W. R. MARTINI. Stirling engine design manual, 2nd edition. Technical report, Martini Engineering, Richland, WA (USA), 1983.
- [52] M. Hooshang, R. Askari Moghadam, and S. AlizadehNia. Dynamic response simulation and experiment for gamma-type stirling engine. *Renewable Energy*, 86:192 – 205, 2016.